Journal of Sound and Vibration (1999) **224**(1), 33–47
Article No. jsvi.1998.2028, available online at http://www.idealibrary.com on IDEAL®

SINGLE-MODE CONTROL OF A CANTILEVER BEAM UNDER PRINCIPAL PARAMETRIC EXCITATION

S. S. Oueini and A. H. Nayfeh
Department of Engineering Science and Mechanics, Virginia Polytechnic Institute and State University, Blacksburg, VA 24061-0219, *U.S.A.*

(*Received* 30 *March* 1998, *and in final form* 27 *October* 1998)

The problem of suppressing the vibrations of a structure that is subjected to a principal parametric excitation is tackled. The vibration amplitudes resulting from such resonance cannot be fully controlled by conventional techniques, such as the addition of linear damping through velocity feedback or by the implementation of conventional mass absorbers. However, it has been shown that the growth of the response is limited by non-linearities. In this work, this fact is capitalized on and a simple non-linear feedback law is devised to suppress the vibrations of the first mode of a cantilever beam when subjected to a principal parametric resonance. The dynamics of the beam are modelled with a second-order non-linear ordinary-differential equation. The model accounts for viscous damping, air drag, and inertia and geometric non-linearities. A control law based on cubic velocity feedback is proposed. The method of multiple scales is used to derive two first-order ordinary-differential equations that govern the time variation of the amplitude and phase of the response. A stability study is conducted and the open- and closed-loop response of the system is analyzed. Furthermore, results are presented of experiments conducted to control the vibrations of a cantilever steel beam fitted with piezoceramic actuators. The theoretical and experimental findings indicate that the control law leads to effective vibration suppression and bifurcation control.

1. INTRODUCTION

Parametric resonance was first observed by Faraday [1]. He noted that a fluid in a vertically oscillating container develops horizontal surface waves. This resonance is peculiar because it occurs when the forcing frequency is close to twice of one of the natural frequencies of the excited system, and it leads to high-amplitude motions. Researchers have since given it considerable attention. The first model exhibiting such a behavior is due to Mathieu [2]. The analysis of this model reveals that, unlike systems subjected to a primary external excitation, viscous damping does not limit the amplitude of the response. The linear damping, however, delays the onset of the instability [3].

In a realistic situation, such as the case of structural vibrations, the growth of the response is limited by non-linearities that are not accounted for by any

0022–460X/99/260033 + 15 $30.00/0

Mathieu-type model. Zavodney *et al*. [4] studied the response of a model that includes quadratic and cubic geometric non-linearities. They found that stable limit cycles can exist. They also showed that the system can exhibit quasi-periodic and chaotic motions. Zavodney and Nayfeh [5] investigated the dynamics of a cantilever beam carrying a lumped mass. They modelled the structure with cubic geometric and inertia non-linearities. They conducted experiments and reported results that were in general agreement with the theory. Anderson *et al*. [6] improved the model proposed by Zavodney and Nayfeh [5] and considered the effect of quadratic damping on the response of the system. Their theoretical results agreed very well with the experiments.

Interesting dynamics have also been investigated in parametrically excited multi-degree-of-freedom systems. Miles [7] analyzed the response of a system of two quadratically coupled oscillators under the condition of exact autoparametric (two-to-one) resonance when the lower mode is excited at twice its natural frequency. Nayfeh [8] extended the work of Miles and found that, for certain detunings, the response of the system is bounded. He also derived conditions under which the system undergoes Hopf bifurcations. Nayfeh and Jebril [9] studied a similar system but included cubic non-linearities. They considered the cases of principal, additive, and simultaneous resonances. More recently, Chin *et al*. [10] analyzed the dynamics of a buckled beam possessing a two-to-one internal resonance when the higher mode is subjected to a principal parametric excitation. They reported the occurrences of Hopf and period-doubling bifurcations, type I intermittency, chaos, and crises.

Asfar and Masoud [11] implemented a Lanchester-type damper to suppress the vibrations of a single-degree-of-freedom system subjected to a principal parametric resonance. They conducted numerical studies and demonstrated effective suppression and bifurcation control. Thomsen [12] considered a string under similar conditions and used a sliding-mass non-linear absorber. His studies reveal that, for moderate forcing amplitudes, successful suppression is possible. For high forcing amplitudes or a large slider mass, the system exhibits modulated responses.

In this paper, the problem of suppressing the vibrations of a cantilever beam when subjected to a principal parametric resonance is considered. The dynamics of the first mode are modelled with a second-order non-linear ordinary-differential equation and a control law based on cubic velocity feedback is introduced. The addition of linear velocity feedback is mathematically equivalent to adding viscous damping and, therefore, will not be effective in reducing the vibration amplitude due to the resonance. However, cubic velocity feedback is equivalent to cubic non-linearities that are known to limit the amplitude of the parametric resonance. The method of multiple scales is used to obtain an approximate solution to the differential equation and the stability of the response is investigated. Then, the results of the perturbation solution are verified through numerical simulations. Additionally, the performance of the control law is investigated through experiments. A cantilever beam fitted with piezoceramic actuators is mounted vertically on a shaker, and a parametric study

is performed to examine the effects of varying the control gain on the closed-loop response of the system.

2. SYSTEM MODEL AND PERTURBATION SOLUTION

A cantilever beam mounted on a shaker and actuated with piezoceramic patches is considered. In non-dimensional form, the dynamics of the first mode of the structure are modelled by

$$\ddot{u} + u + 2\varepsilon\mu_1\dot{u} + \varepsilon\hat{\mu}_2|\dot{u}|\dot{u} + \varepsilon\alpha_1 u^3 + \varepsilon\alpha_2 u^2\ddot{u} + \varepsilon\alpha_3 u\dot{u}^2 = \varepsilon u F\cos(\Omega t) + T, \quad (1)$$

where u is the generalized co-ordinate, μ_1 is the viscous damping coefficient, $\hat{\mu}_2$ is the air drag coefficient, the α_i are constants, F and Ω are the forcing amplitude and frequency, respectively, T is a control input, and ε is a non-dimensional bookeeping parameter. The term $\alpha_1 u^3$ is due to non-linear curvature, and the terms $\alpha_2 u^2\ddot{u}$ and $\alpha_3 u\dot{u}^2$ are due to non-linear inertia [5].

The case of principal parametric resonance (i.e., $\Omega \approx 2$) is considered and a control law given by

$$T = -\varepsilon G_v \dot{u}^3, \quad (2)$$

is proposed, where G_v is a positive constant.

To analyze the solutions of equations (1) and (2), the method of multiple scales is used [13] and u is expanded as

$$u(T_0, T_1) = u_0(T_0, T_1) + \varepsilon u_1(T_0, T_1) + \cdots, \quad (3)$$

where T_0 is a fast time scale and T_1 is a slow time scale describing variations in the amplitude and phase of the response. The time derivatives are recast in terms of the new time scales as

$$\frac{\mathrm{d}}{\mathrm{d}t} = D_0 + \varepsilon D_1 + \cdots \quad \text{and} \quad \frac{\mathrm{d}^2}{\mathrm{d}t^2} = D_0^2 + 2\varepsilon D_0 D_1 + \cdots, \quad (4)$$

where $D_k \equiv \partial/\partial T_k$. Substituting equations (3) and (4) into equations (1) and (2) and equating coefficients of like power of ε yields

$O(1)$:

$$D_0^2 u_0 + u_0 = 0, \quad (5)$$

$O(\varepsilon)$:

$$\begin{aligned} D_0^2 u_1 + u_1 = {} & -2D_0 D_1 u_0 - 2\mu_1 D_0 u_0 - \hat{\mu}_2 |D_0 u_0| D_0 u_0 - \alpha_1 u_0^3 \\ & - \alpha_2 u_0^2 D_0^2 u_0 - \alpha_3 u_0 (D_0 u_0)^2 - G_v (D_0 u_0)^3 + u_0 F\cos(\Omega T_0). \end{aligned} \quad (6)$$

The solution of equation (5) can be expressed as

$$u_0 = A(T_1)\,\mathrm{e}^{iT_0} + \bar{A}(T_1)\,\mathrm{e}^{-iT_0}, \quad (7)$$

where $A(T_1)$ is a complex-valued quantity that will be determined by imposing the solvability condition at the next level of approximation.

To express the nearness of Ω to 2, a detuning parameter σ such that

$$\Omega = 2 + \varepsilon\sigma. \tag{8}$$

Substituting equations (7) and (8) into equation (6) and eliminating the terms that produce secular term leads to

$$2i(D_1A + \mu_1 A) + \frac{\hat{\mu}_2}{2\pi}\int_0^{2\pi} D_0u_0|D_0u_0|\,\mathrm{e}^{-iT_0}\,\mathrm{d}T_0 + 8(\alpha_e + i\mu_3)A^2\bar{A} - 2\bar{A}f\,\mathrm{e}^{i\sigma T_1} = 0, \tag{9}$$

where

$$\alpha_e = \frac{1}{8}(3\alpha_1 - 3\alpha_2 + \alpha_3),\ \mu_3 = \frac{3G_v}{8}, \quad \text{and} \quad f = \frac{F}{4}.$$

Next, A is expressed in the polar form

$$A = \tfrac{1}{2}a(T_1)\,\mathrm{e}^{i\beta(T_1)}. \tag{10}$$

Inserting equation (10) into equation (9), performing the integration, and separating real and imaginary parts yields

$$a' = -\mu_1 a - \mu_2 a^2 - \mu_3 a^3 + af\sin\theta, \tag{11}$$

$$a\theta' = \sigma a - 2\alpha_e a^3 + 2af\cos\theta, \tag{12}$$

where the prime denotes differentiation with respect to T_1,

$$\theta = \sigma T_1 - 2\beta \quad \text{and} \quad \mu_2 = \frac{4\hat{\mu}_2}{3\pi}.$$

3. PERFORMANCE OF THE CONTROL LAW

The performance of the control technique is evaluated by calculating the equilibrium solutions (fixed points) of equations (11) and (12) and examining their stability as a function of the parameters f and σ and the gain $G_v(\mu_3)$. Setting $a' = 0$ and $\theta' = 0$ yields

$$af\sin\theta = \mu_1 a + \mu_2 a^2 + \mu_3 a^3, \tag{13}$$

$$-af\cos\theta = \tfrac{1}{2}\sigma a - \alpha_e a^3. \tag{14}$$

There are two possibilities: $a = 0$ and $a \neq 0$. The non-trivial fixed points are given by the roots of

$$(\mu_1 + \mu_2 a + \mu_3 a^2)^2 + (\tfrac{1}{2}\sigma - \alpha_e a^2)^2 - f^2 = 0, \tag{15}$$

and

$$\tan\theta = \frac{2(\mu_1 + \mu_2 a + \mu_2 a^2)}{2\alpha_e a^2 - \sigma}. \tag{16}$$

The stability of the non-trivial fixed points is investigated by evaluating the eigenvalues of the Jacobian matrix of equations (11) and (12). In the case of the trivial solution, the form of these equations is not suitable for the stability analysis. Therefore, A is expressed in the Cartesian form

$$A = \tfrac{1}{2}(p - iq)\, e^{\nu T_1}, \tag{17}$$

where p and q are real and $\nu = \frac{1}{2}\sigma$. Substituting equation (17) into equation (9) yields

$$p' = -\mu_1 p - \mu_2 p\sqrt{p^2 + q^2} - \mu_3 p(p^2 + q^2) - \nu q + \alpha_e q(p^2 + q^2) + qf, \tag{18}$$

$$q' = -\mu_1 q - \mu_2 q\sqrt{p^2 + q^2} - \mu_3 q(p^2 + q^2) + \nu p - \alpha_e p(p^2 + q^2) + pf. \tag{19}$$

The stability of the trivial solution ($p = q = 0$) to a disturbance proportional to $e^{\lambda T_1}$ is ascertained by the roots of

$$\begin{vmatrix} -\mu_1 - \lambda & -\nu + f \\ \nu + f & -\mu_1 - \lambda \end{vmatrix} = 0, \tag{20}$$

whose solution is

$$\lambda = -\mu_1 \pm \sqrt{f^2 - \nu^2}. \tag{21}$$

The trivial solution is stable if

$$f \leqslant \sqrt{\mu_1^2 + \nu^2}, \tag{22}$$

when f is the control parameter, or if

$$|\sigma| \geqslant 2\sqrt{f^2 - \mu_1^2}, \tag{23}$$

when σ is the control parameter.

Due to the complexity in obtaining a closed-form solution to equation (15), numerical methods are used to investigate the stability of the non-trivial solutions. In the next three sections, the stability analysis is performed and the control law is evaluated.

3.1. FREQUENCY–RESPONSE CURVES

Figure 1 shows the frequency–response curves of the open- and closed-loop system. The amplitude of the response depends on the value of σ and the system's initial conditions.

First, the open-loop response (i.e., $G_v = 0$) is considered. When $\sigma > \sigma_B$, only the trivial solution exists. As σ is decreased from point A, the trivial solution

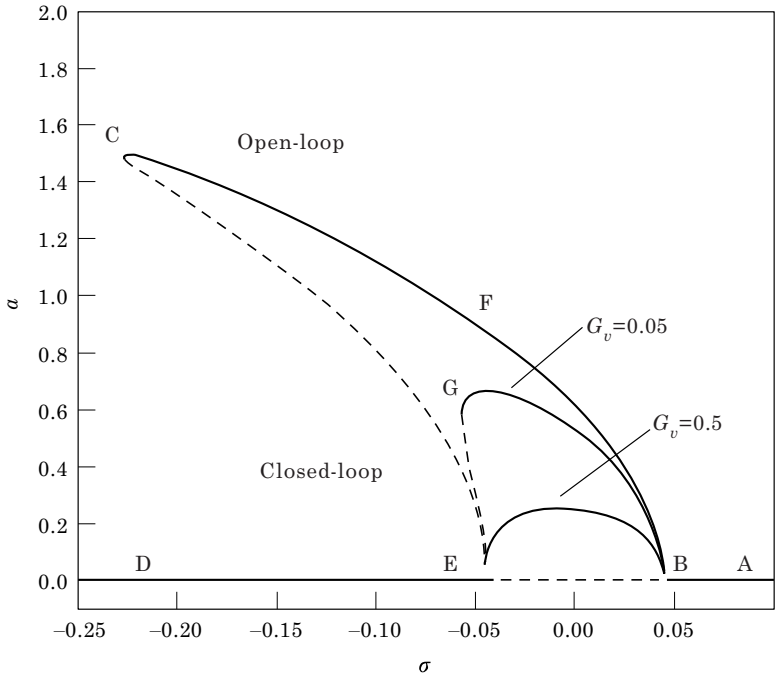

Figure 1. Theoretical frequency–response curves when $f=0{\cdot}025$, $\mu_1=0{\cdot}01$, $\mu_2=0{\cdot}01$, and $\alpha_e=-0{\cdot}05$; (—) stable solution (– –) unstable solution.

looses stability at point B through a transcritical bifurcation. The response amplitude increases as σ is decreased. The solution loses stability through a saddle-node bifurcation at point C, and the response amplitude jumps down to point D where only the trivial solution exists thereafter. In the case where σ is increased, there are two possible paths for the solution. If the initial conditions are small, the system does not oscillate initially, and the response traces the curve DE. When point E is reached, the trivial solution loses stability through a transcritical bifurcation, and the resulting non-trivial solution quickly encounters a saddle-node bifurcation, leading to a jump to point F. Upon further increasing σ, the amplitude traces the curve FBA, where the trivial solution is reached through a supercritical pitchfork bifurcation at point B. If the initial conditions are large, a high-amplitude response is sustained initially. Here, a jump phenomenon does not occur, and the response traces portions of or all the curve CFBA. Note that the overhang region FC exhibits high-amplitude responses.

Next, the response of the closed-loop system (i.e., $G_v\neq 0$) is analyzed. Two cases are considered, $G_v=0{\cdot}05$ and $G_v=0{\cdot}5$. In the first case, the response undergoes bifurcations similar to those of the open-loop system. However, the response amplitude is decreased, and the saddle-node bifurcation is shifted from point C to point G. In the second case, superior results are achieved. The saddle-node bifurcation is replaced with one transcritical bifurcation at point E. The overhang region and the jump phenomenon are eliminated, and the response is suppressed further.

3.2. FORCE–RESPONSE CURVES

Figure 2 shows the open- and closed-loop force–response curves. Since an exact resonance ($\sigma = 0$) is difficult to achieve realistically, a response curve is shown that exhibits the more interesting hysteretic effect when $\sigma < 0$.

First, the open-loop response is considered. If $f < f_E$, only the trivial solution exists. In the absence of large disturbances, it is maintained as f is increased along the curve AB. When f reaches the value at point B, the trivial solution loses stability through a transcritical bifurcation, and the resulting non-trivial solution quickly encounters a saddle-node bifurcation, leading to a jump to point C. A further increase in f leads to higher response amplitudes tracing the curve CD. When f is decreased, the amplitude traces the curve DE. At point E, the solution undergoes a saddle-node bifurcation, leading to a jump down where only the trivial solution exists thereafter.

Second, the response for two values of the feedback gain is analyzed. When $G_v = 0{\cdot}05$, the response curve is similar to the uncontrolled response curve. The bifurcations are identical, however; the location of the saddle-node bifurcation point is shifted from point E to point H, resulting in a smaller hysteretic region. Furthermore, the response amplitude is reduced from the curve ECD to the curve HFG. When $G_v = 0{\cdot}5$, the saddle-node bifurcations are replaced with one transcritical bifurcation at point B. Additionally, the amplitude of the response is further reduced.

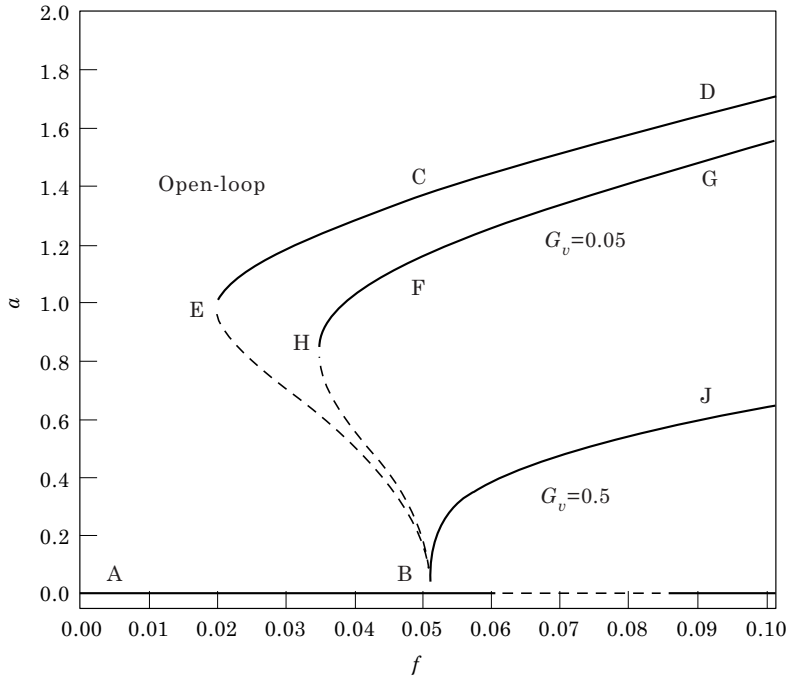

Figure 2. Theoretical force–response curves when $\sigma = -0{\cdot}1$, $\mu_1 = 0{\cdot}01$, $\mu_2 = 0{\cdot}01$, and $\alpha_e = -0{\cdot}05$; —, stable solution; – –, unstable solution.

3.3. NUMERICAL SIMULATIONS

To validate the perturbation results, the equation

$$\ddot{u} + u + 2\mu_1\dot{u} + \tfrac{3}{4}\pi\mu_2|\dot{u}|\dot{u} + \tfrac{8}{3}\alpha_1 u^3 = Fu\cos(\Omega t) - G_v\dot{u}^3, \tag{24}$$

was integrated numerically, where $\mu_1 = 0{\cdot}01$, $\mu_2 = 0{\cdot}01$, $\alpha_1 = -0{\cdot}05$, $\alpha_2 = \alpha_3 = 0$, and $F = 0{\cdot}1$ for different values of the forcing frequency Ω and the velocity feedback gain G_v. Figure 3 shows time responses when $\Omega = 2$ (i.e., $\sigma = 0$) for $G_v = 0{\cdot}05$ and $G_v = 0{\cdot}5$. Comparing Figures 1 and 3, it is noted that the open- and closed-loop response amplitudes predicted by the perturbation solution are in agreement with the results of the numerical simulations. Figure 4 shows results when $\Omega = 1{\cdot}9$ (i.e., $\sigma = -0{\cdot}1$) for $G_v = 0{\cdot}05$ and $G_v = 0{\cdot}5$. In this case, the system possesses two stable states: the trivial solution and a high-amplitude limit-cycle solution (the system is operating in the overhang region CF shown in Figure 1). Thus, the initial conditions for this simulation are chosen to insure that the system is attracted to the non-trivial solution. Here, the addition of velocity feedback eliminates the high-amplitude motion. Since only the trivial solution exists, the amplitude of the closed-loop response is not influenced by the magnitude of the gain G_v. However, the gain affects the transient behavior. The higher the gain is, the faster is the approach to the trivial solution.

4. EXPERIMENTS

The theoretical analysis is verified by implementing the control strategy on a cantilever beam fitted with piezoceramic actuators and a strain gage. The beam is excited vertically by a shaker subjecting its first mode to a principal parametric resonance.

4.1. SETUP

The properties of the beam and the actuators are listed in Table 1. The natural frequency of the first mode was approximately 7 Hz. The clamping fixture and

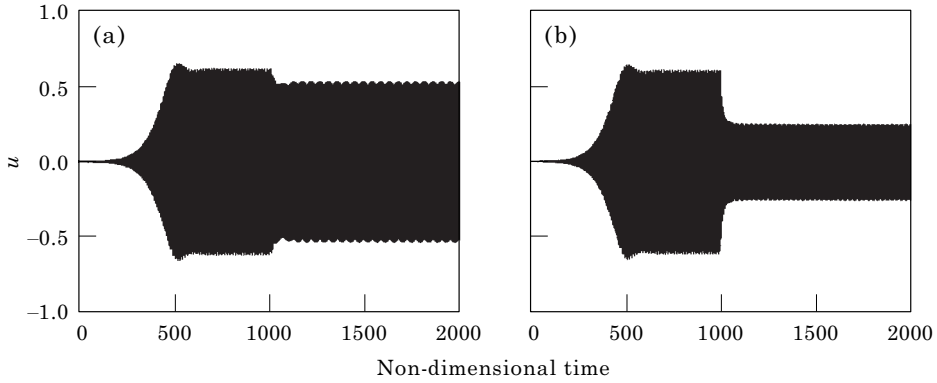

Figure 3. Numerical simulations of the time response when $\Omega = 2$: (a) $G_v = 0{\cdot}05$ and (b) $G_v = 0{\cdot}05$.

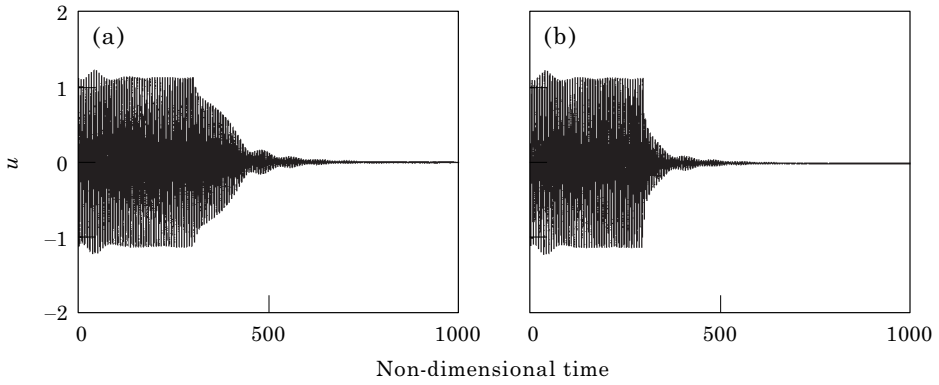

Figure 4. Numerical simulations of the time response when $\Omega = 1{\cdot}9$: (a) $G_v = 0{\cdot}05$ and (b) $G_v = 0{\cdot}5$.

the configuration of the actuators and the strain gage are shown in Figure 5. An accelerometer is positioned on the shaker head to measure the forcing amplitude. The set-up for the experiment is shown in Figure 6. The beam and clamping fixture are attached to a 100 lb permanent-magnet shaker that is driven through a signal generator and a power amplifier. The signal from the strain gage is filtered and sampled by a digital computer using the software LabView. The signal is manipulated, and the cubic velocity signal is generated, amplified, and then sent to the actuators.

4.2. FREQUENCY–RESPONSE CURVES

The beam was forced at 1·2 *g* and forward and reverse frequency sweeps were conducted. The acceleration of the shaker head was monitored, and the input voltage driving the shaker was adjusted to maintain a constant forcing amplitude. Figure 7 exhibits the open- and closed-loop frequency–response curves.

First, the open-loop case is presented. Initially, as the forcing frequency was increased, the amplitude remained at zero. When the frequency reached a value close to 13·9 Hz, the response jumped up to a value of 0·3 V. Further increases in the frequency led to a decrease in the amplitude. When the frequency was approximately 14·1 Hz, the beam stopped oscillating. Subsequently, the response remained at zero. In the reverse sweep, the response was similar to the one

TABLE 1

Properties of beam and actuators

	Beam	Actuators
Length (m)	0·26	0·03
Width (m)	$1{\cdot}3 \times 10^{-2}$	
Thickness (m)	$6{\cdot}0 \times 10^{-4}$	$1{\cdot}9 \times 10^{-4}$
Elastic modulus (GPa)	208	6·20
Strain coefficient (m/V)	N/A	-190×10^{-12}

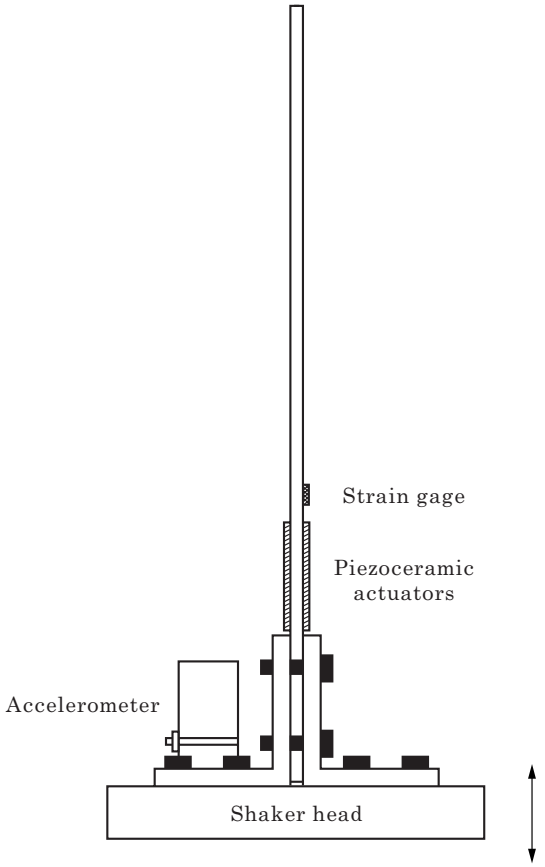

Figure 5. Beam fixture and instrumentation.

observed during the forward sweep. However, the response amplitude did not experience a jump down at 13·9 Hz. Instead, a growth rate was observed, leading to a very high response amplitude reaching 2·9 V. A jump down to zero occurred at 13·6 Hz. Thereafter, the response remained at zero.

Second, the closed-loop case is considered. As the frequency was increased, the response remained at zero until a gradual increase was observed at 13·9 Hz. Further increases in the frequency resulted in a decrease in the response amplitude leading to a zero response at 14·1 Hz. During the reverse sweep, the response amplitude traced the same path observed during the closed-loop forward sweep. The high-amplitude motion attained in the open-loop system was eliminated.

4.3. FORCE–RESPONSE CURVES

The beam was forced at a constant frequency of 13·88 Hz and forward and reverse force sweeps were conducted. Figure 8 shows the open- and closed-loop force–response curves.

First, the open-loop response is described. As the force was increased, the beam did not oscillate initially. When the forcing amplitude reached approximately 1·5 g, the response experienced a jump to a high amplitude

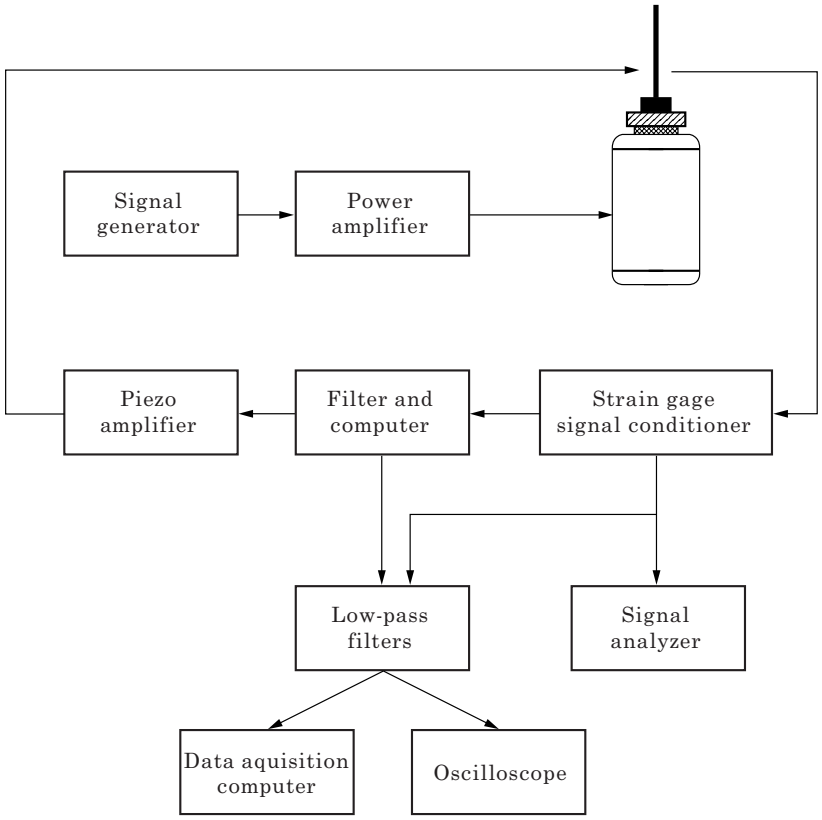

Figure 6. The experimental set-up.

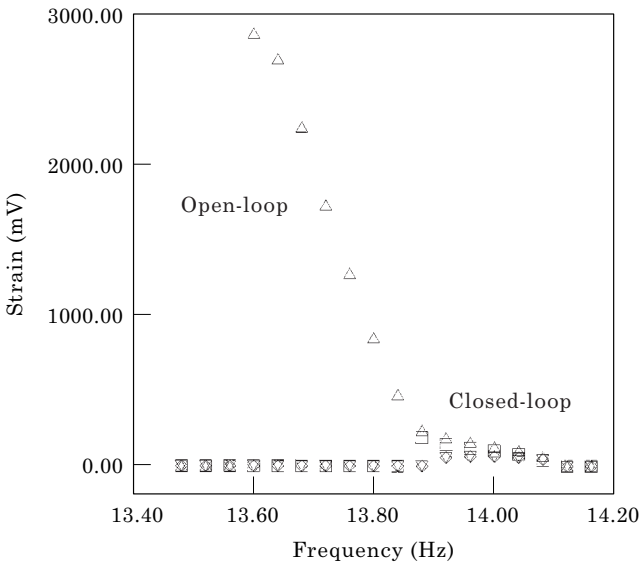

Figure 7. Experimental open- and closed-loop frequency–response curves. Open-loop: □, forward sweep; △, reverse sweep. Closed-loop: ▽, forward sweep; ◇, reverse sweep.

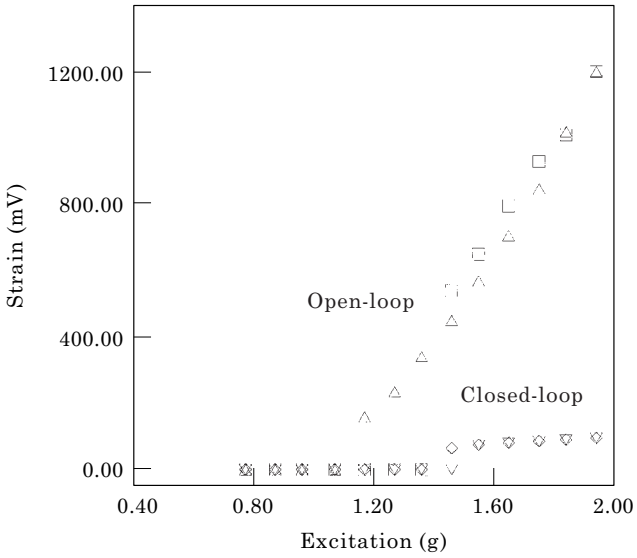

Figure 8. Experimental open- and closed-loop force–response curves. Open-loop: □, forward sweep; △, reverse sweep. Closed-loop: ▽, forward sweep; ◇, reverse sweep.

(0·5 V). Further increases in the force led to an increase in the response. During the reverse sweep, the response amplitude decreased until a jump down to zero was observed at approximately 1·2 g. The response remained at zero as the forcing was further decreased.

Second, the closed-loop response is examined. As the forcing increased, the beam remained motionless until the forcing amplitude reached 1·5 g. Subsequently, the response amplitude gradually increased, but the amplitude was significantly smaller than in the open-loop case. In the reverse sweep, the amplitude of the response traced identically the response observed in the forward-sweep. However, a very small hysteresis area was observed around 1·5 g.

4.4. EFFECT OF VARYING THE FEEDBACK GAIN

Figures 9–11 compare the response curves and time traces for two feedback gains that differ by an order of magnitude. The gain K shown in the figures is proportional to the gain G_v. The curves labelled "$K=10$" in Figures 9 and 10 correspond to the ones labelled "Closed-loop" in Figures 7 and 8, respectively. In both figures, increasing the gain resulted in a decrease in the response amplitudes. In the case of the force–response curves, increasing the gain led to a more noticeable reduction in the hysteretic region.

In order to examine the transient characteristics of the control law, the beam was subjected to a forcing of 1·2 g at 13·8 Hz. Since the system was operating in the overhang region, the closed-loop response amplitude was expected to be zero. Figure 11 illustrates two time traces for $K=1$ and $K=10$. Clearly, increasing the feedback gain resulted in better transient performance.

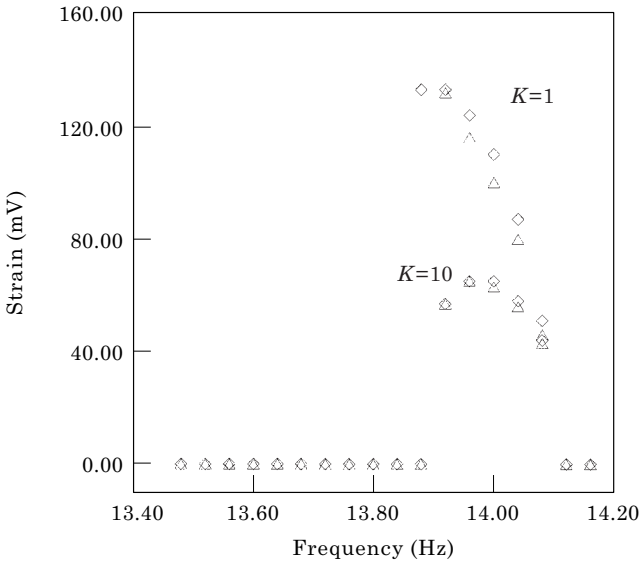

Figure 9. Effect of varying the feedback gain on the frequency–response curve: △, forward sweep; ◇, reverse sweep

5. CONCLUSIONS

A non-linear control law is proposed to suppress the vibrations of the first mode of a cantilever beam when subjected to a principal parametric excitation. The dynamics of the first flexural mode are modelled by a second-order non-linear ordinary-differential equation, and a control law based on cubic velocity

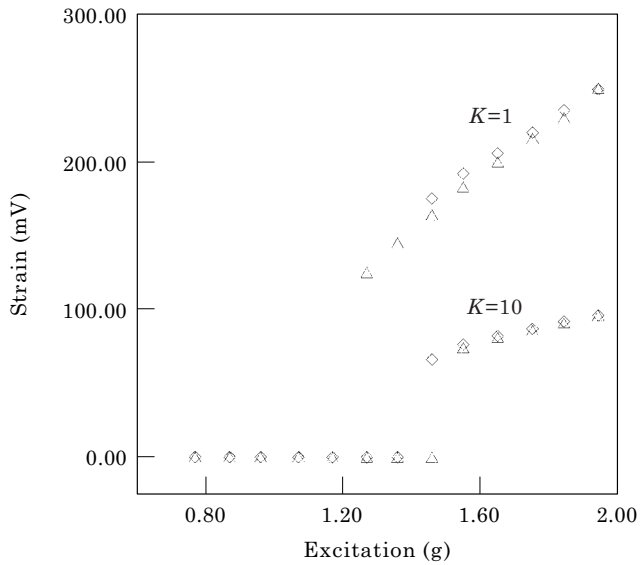

Figure 10. Effect of varying the feedback gain on the force–response curve: ◇, forward sweep; △, reverse sweep.

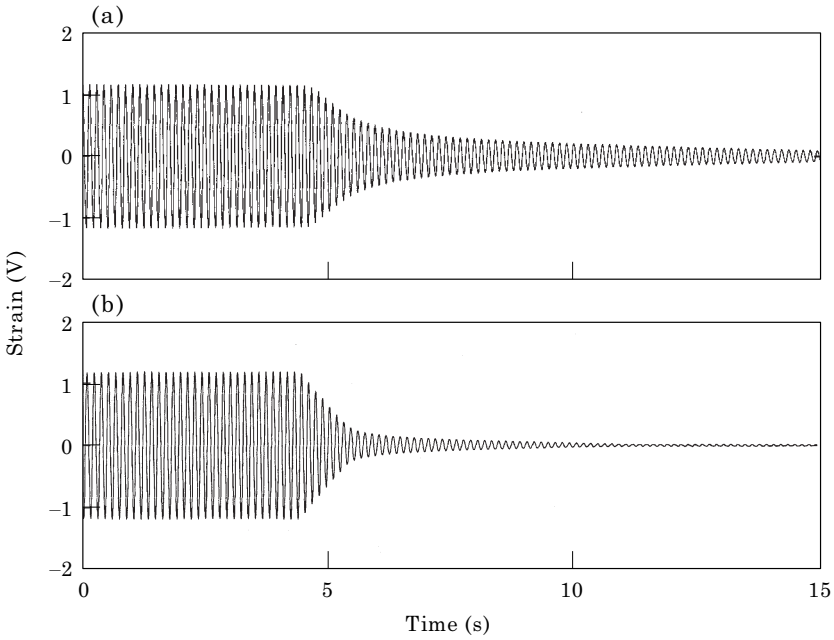

Figure 11. Transient time response: (a) $K = 1$ and (b) $K = 10$.

feedback is introduced. The method of multiple scales is used to derive two first-order differential equations governing the time evolution of the amplitude and phase of the response. Then, a bifurcation analysis is conducted to examine the stability of the closed-loop system and investigate the performance of the control law.

The analysis reveals that cubic velocity feedback reduces the amplitude of the response. Furthermore, it leads to the elimination of the saddle-node bifurcations in the frequency– and force–response curves. These undesirable bifurcations are replaced with transcritical bifurcations. It is further shown that increasing the velocity feedback gain results in better transient performance.

The theoretical analysis is verified experimentally. A cantilever steel beam is fitted with piezoceramic actuators and subjected to a parametric excitation having a frequency equal to twice the natural frequency of its first mode. A computer and a series of analog filters are utilized to generate the cubic velocity feedback signal. The experimental frequency– and force–response curves are in excellent qualitative agreement with the theoretical results.

ACKNOWLEDGMENT

This research was supported by the Army Research Office/NCA&T State University under Grant No. 4–41129–SC–001.

REFERENCES

1. M. FARADAY 1831 *Philosophical Transactions of the Royal Society of London* **121**, 299–318. On a peculiar class of acoustical figures and on certain forms assumed by a group of particles upon vibrating elastic surfaces.
2. E. MATHIEU 1868 *Journal de Mathématiques Pures et Appliquées* **13**, 137–203. Mémoire sur le mouvement vibratoire d'une membrane de forme elliptique.
3. A. H. NAYFEH and D. T. MOOK 1979 *Nonlinear Oscillations*. New York: Wiley.
4. L. D. ZAVODNEY, A. H. NAYFEH and N. E. SANCHEZ 1989 *Journal of Sound and Vibration* **129**, 417–442. The response of a single degree-of-freedom system with quadratic and cubic non-linearities to a principal parametric resonance.
5. L. D. ZAVODNEY and A. H. NAYFEH 1989 *International Journal of Non-Linear Mechanics* **24**, 105–125. The non-linear response of a slender beam carrying a lumped mass to a principal parametric excitation: theory and experiment.
6. T. J. ANDERSON, A. H. NAYFEH and B. BALACHANDRAN 1996 *Journal of Vibration and Acoustics* **118**, 21–27. Experimental verification of the importance of the non-linear curvature in the response of a cantilever beam.
7. J. MILES 1985 *Journal of Applied Mathematical Physics* **36**, 337–345. Parametric excitation of an internally resonant double pendulum.
8. A. H. NAYFEH 1987 *Journal of Sound and Vibration* **119**, 95–109. Parametric excitation of two internally resonant oscillators.
9. A. H. NAYFEH and A. E. S. JEBRIL 1987 *Journal of Sound and Vibration* **115**, 83–101. The response of two degree-of-freedom systems with quadratic and cubic non-linearities to multi-frequency parametric excitations.
10. C. CHIN, A. H. NAYFEH and W. LACARBONARA 1997 *AIAA Paper No*. 97-1081. Two-to-one internal resonances in parametrically excited buckled beam.
11. K. R. ASFAR and K. K. MASOUD 1994 *International Journal of Non-Linear Mechanics* **29**, 421–428. Damping of parametrically excited single-degree-of-freedom systems.
12. J. J. THOMSEN 1996 *Journal of Sound and Vibration* **197**, 403–425. Vibration suppression by using self-arranging mass: effects of adding restoring force.
13. A. H. NAYFEH 1973 *Perturbation Methods*. New York: Wiley.